Jestr

Journal of Engineering Science and Technology Review 16 (4) (2023) 66 - 76

Research Article

JOURNAL OF
Engineering Science and Technology Review

www.jestr.org

Study on Breakdown Process of High -Voltage Pulse Discharge under Water based on Equivalence Theory and Numerical Simulation

Dong Yan[1,2,3,4], Lipeng Lai[1,*], Xuedang Xiao[2], Lei Zhang[4] and Inchen Chen [5]

[1]*College of Architecture and Civil Engineering, Xinyang Normal University, Xinyang, 464000, China*
[2]*Xinyang Lingshi Technology Co., Ltd, Xinyang, 464000, China*
[3]*Henan New Environmentally-Friendly Civil Engineering Materials Engineering Research Center, Xinyang Normal University, Xinyang, 464000, China*
[4]*Yellow River Institute of Hydraulic Research, YRCC, Zhengzhou, 450003, China*
[5]*International College, Krirk University, Bangkok 10220, Thailand*

Received 7 April 2023; Accepted 10 July 2023

Abstract

The breakdown process of high-voltage pulse discharge under water involves rapid changes in the plasma channel, which are influenced by various factors, such as time, electric field, and thermal field. Accurately measuring the plasma channel is challenging due to technological limitations. This study proposed the theory of equivalence and equivalent numerical simulation for underwater pulsed discharge to understand the breakdown process and the role of the plasma channel in high-voltage pulse discharge under water. It established the equivalence theory and numerical simulation of the discharge breakdown process by considering the delay characteristics of discharge breakdown and the plasma channel model. The plasma channel was described intuitively and quantitatively, providing a concise and effective analysis of the complex breakdown process. Results indicate that (1) the breakdown channel undergoes an initial plasma channel stage accompanied by heating effects, which then transforms into an arc channel, leading to breakdown and detonation. (2) The equivalent resistance of the plasma channel is approximately 10 Ω, and the equivalent radius of the initial channel is around 0.1 μm. Breakdown is difficult to achieve when the electrode spacing is 0.5 cm and the charging voltage Um is below 5.5 kV, with an estimated minimum charging voltage of approximately 6 kV required for breakdown. (3) Equivalence theory enables effective quantification of the equivalent radius and equivalent resistance in the breakdown process, providing a representative measure of breakdown process stability. It proves to be an effective method for monitoring the operation of discharge equipment in practical engineering. The study provides a reliable reference for assessing the breakdown process of underwater high-voltage pulse discharge and monitoring the performance of pulse discharge equipment.

Keywords: Pulsed discharge underwater; Breakdown process; Plasma channel; Equivalence theory; Numerical simulation

1. Introduction

The process of high-voltage pulse discharge in water involves a range of complex phenomena, including mechanical, electrical, thermal, and electrochemical effects. In engineering applications, the breakdown characteristics of high-voltage pulse discharge are of primary importance. Scholars have empirically summarized the long-term breakdown delay in discharge studies. Achieving arc discharge requires injecting sufficient electrical energy into the water medium between the electrodes, leading to gasification and gradual gasification-ionization process. The breakdown model of the water medium is often described as a "gasification model" with characteristics of "electron collision" ionization. The process can be described as follows: localized field emission current from the electrode surface heats the water medium, causing gasification and the formation of small bubbles, which enhance the local breakdown effect of the electric field. High temperature charged particles are generated, and they accelerate and impact the boundary of the water medium under the action of the electric field, resulting in heating and gasification. The gasified water molecules are continuously ionized by the impact of electrons. The ionized electrons, driven by the electric field, continue to strike the boundary water medium, forming a cycle of "gasification-ionization." This process extends to the other electrode, where it forms a bright plasma channel and causes breakdown. Zhu [1] proposed that the passage where the "gasification-ionization" cycle occurs is known as a streamer [2] during the "gasification-ionization" process. In essence, this channel represents a plasma channel. Figure 1 depicts a schematic of the streamer generation and connection process based on the "gasification-ionization model" breakdown.

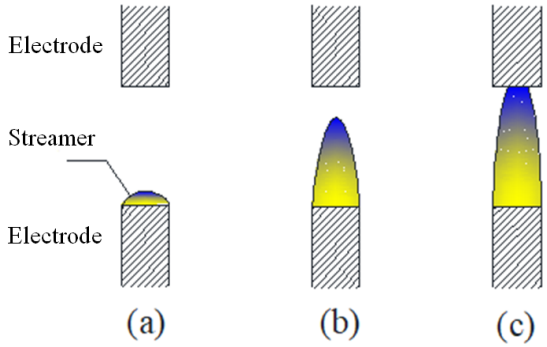

Fig. 1. Schematic of the streamer generation and connection process

*E-mail address: lai201510@163.com
ISSN: 1791-2377 © 2023 School of Science, IHU. All rights reserved.
doi:10.25103/iestr.164.09

In Fig. 1, (a) represents the initial formation stage of the streamer, (b) represents the extension and development stage of the streamer during the "gasification-ionization" cycle, and (c) represents the streamer extending to the other electrode, forming a complete path. Scholars have explained the phenomenon of long-duration breakdown, but the involvement of multiple factors and technical challenges have hindered a comprehensive understanding of the breakdown process and its quantification in theory. Therefore, effectively grasping the fundamental aspects of the breakdown process, simplifying the analysis process, and clarifying the relevant theoretical foundations are crucial.

This study conducts equivalent theoretical research on the breakdown process of underwater pulsed discharge through a combination of experiments and theoretical approaches. It provides a detailed theoretical analysis of the equivalent breakdown process and establishes numerical and simulation models to analyze the plasma channel throughout the breakdown process. The objective of this research is to quantitatively study the plasma channel in the breakdown process of underwater pulsed discharge and provides insights into the development and optimization of underwater pulsed discharge technology.

2. State of the art

Extensive studies have been conducted by scholars on underwater pulsed discharge technology. Touya [3] obtained relevant mechanical parameters of underwater pulsed discharge through experimental research and proposed the theory and empirical formula for shock wave peak pressure. However, the limited number of experimental data collection points requires additional observation points. Chen and Olivier [4] indicated that underwater pulsed discharge technology can effectively replace hydraulic fracturing in low permeability oil and gas reservoirs to enhance permeability and production. However, they did not address the mechanical energy effect of underwater pulsed discharge. Bruggeman [5] and colleagues described high-voltage pulsed discharge breakdown in water as a unique plasma physical phenomenon. Although the breakdown process involves various physical processes, including mechanics, heat, and electricity, a corresponding description of the mechanical action characteristics during the breakdown process is lacking. Ahmad [6, 7] focused on the fundamental physical phenomena of low-heat plasma generated by pulsed discharge at standard atmospheric pressure. They monitored the electrical and optical properties of the discharge using probes and ultra-high-speed imaging, respectively, and conducted adequate experimental research. However, mechanical analysis of pulsed discharge plasma was lacking. Rond [8] conducted experimental research on pulsed plasma discharge in water using a needle electrode configuration. They investigated the phenomena before and after underwater pulsed discharge breakdown and measured various electrical parameters. Thomas [9] determined the equivalent circuit of plasma through discharge experiments, obtaining discharge characteristics and the relationship between voltage and current. They discovered that plasma resistance is time-dependent, whereas inductance is not. Rober [10] evaluated the influence of output voltage setting using a continuous-flow liquid film reactor powered by a variable nanosecond pulse power supply, but analysis of relevant physical and mechanical properties was lacking.

Lu [11-13] conducted extensive research on plasma experiments, particularly focusing on the physical properties of plasma in underwater high-voltage pulse discharge experiments. The characteristics of pulsed discharge plasma at atmospheric pressure were discussed. Sun [14-16] introduced a pulse discharge source capable of arc discharge and corona discharge to investigate the discharge characteristics under different conditions and discussed the basic application research related to the electrohydraulic effect. Zhou [17] provided a brief introduction to the discharge process and analyzed the characteristics of solid water under difference load conditions. Duan [18] conducted numerous experiments to investigate the electrochemical phenomena associated with the generation of TiO2 carriers and the process of interfacial charge transfer in an underwater pulsed discharge plasma system. His research aimed to understand the influence of chemical and physical effects on these phenomena. Yan [19] conducted an underwater pulsed discharge experiment to investigate the characteristics of shock wave generation and attenuation under hydrostatic pressure using, and the mechanical properties associated with it. However, relevant theoretical analysis was lacking in their study.

The aforementioned studies primarily focused on experimental pulse discharge technology with limited emphasis on the equivalence theory of the breakdown process, particularly in terms of theoretical simulation research throughout the entire process. This study aims to address this gap by establishing a numerical simulation model based on experimental research and theoretical analysis, specifically targeting the exploration of the equivalence theory. This study reveals the functional characteristics of the breakdown form and explains the underlying physical processes by analyzing the experimental results and studying the thermal effect process of the discharge. The findings of this study provide a reliable reference for the utilization of underwater high-voltage pulse discharge technology.

The remainder of this study is organized as follows. The third section describes the experimental content of underwater high-voltage pulse discharge and the construction of the numerical simulation model. The fourth section examines the equivalence theory using experimental results and simulations, explaining the entire physical process and investigating its practical application. The study concludes with summary and relevant conclusions.

3. Methodology

3.1 Experiment

The experimental equipment consists of an underwater pulsed discharge device and a precision measurement system. Figure 2 shows a schematic of the underwater pulsed discharge experimental system. The pulsed power supply can provide DC high voltage ranging from 6 kV to 15 kV, with a rated capacitance of 60 μF and a maximum energy of storage of 7000 J. A photograph of the actual electrical power unit with high-voltage pulse is shown in Figure 3. The structure diagram and photograph of the electrode construction are shown in Figure 4. The electrodes are made of steel pipes and copper rods, and the distance between the positive and negative electrodes is 5 mm. The electrodes are placed at the head of a pipe with an inner diameter of 100 mm and a length of 4 m, and static water pressure is provided by a pressure pump.

In the experiment, the transient pulse voltage waveform was measured using a combination of the P6015A high-voltage probe and DSO6014A digital oscilloscope. The P6015A high-voltage probe, manufactured by Tektronix, is commonly used for measuring voltages below 40 kV. It has an attenuation ratio of 1000×, compensation range of 7-49 pF, bandwidth of 75 MHz, and is suitable for measuring transient pulse voltages above 2.5 kV. For measuring transient current, a widely used current measuring coil, known as a Rogowski coil, was employed. The Rogowski coil is based on the principles of electromagnetic induction and the law of total current, and it was developed by the Institute of Electrician Engineering, Chinese Academy of Sciences.

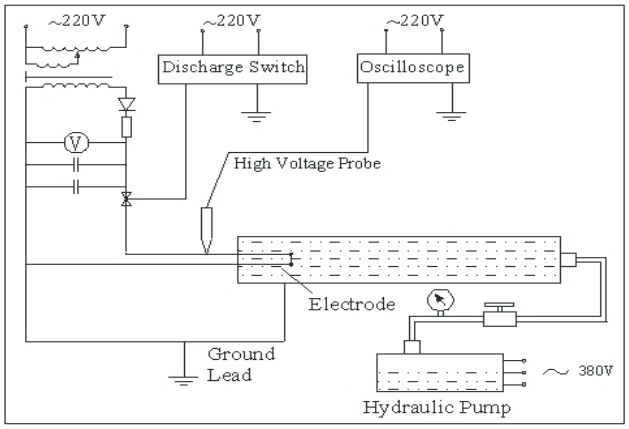

Fig. 2. Picture of the actual electrical power unit with high-voltage pulse used in this work

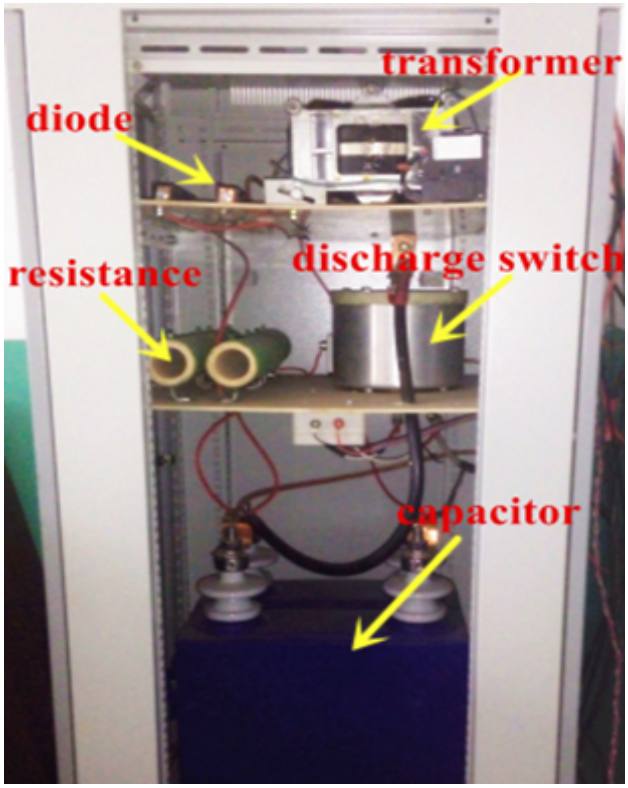

Fig. 3. Picture of the actual electrical power unit with high-voltage pulse used in this work

During the experiment, the pipeline was filled with tap water, with a conductivity of approximately 1.25 S/m. The charging voltage *Um* is varied at four different levels: 9, 11, 13, and 15 kV. The experimental data under different charging voltages and hydrostatic pressures were obtained through experiments. These experimental results, combined with theoretical research, allowed for the discussion of the equivalence theory and simulation of underwater pulsed discharge breakdown, and the proposal of a practical application scheme.

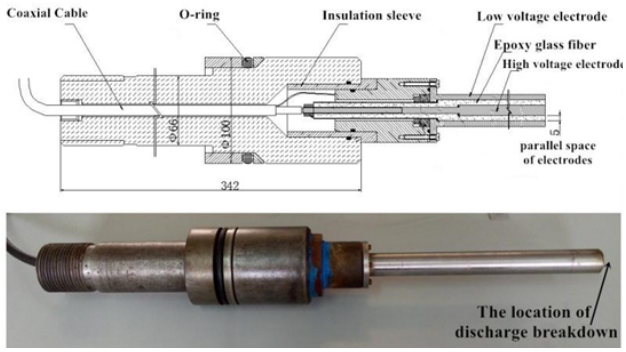

Fig. 4. Picture of the actual electrode and its structural diagram

3.2 Experimental protective measures

The experiment mainly focuses on studying the breakdown characteristics of underwater pulsed discharge. The Rogowski coil, P6015A high-voltage probe and DSO6014A oscilloscope are utilized to accurately collect transient voltage and current data. During the experiment, the whole experimental pipeline is filled with tap water, which has a conductivity of approximately 1.2 S/m. The charging voltage Um can be adjusted within the range of 5 kV to 15 kV, and the electrode gap is set at 5 mm. The time-history curves of breakdown voltage and breakdown current under different charging voltages can be obtained by conducting experiments. Combined with theoretical analysis and numerical simulation, the electrical characteristics and equivalence theory of discharge breakdown in water are investigated.

During the experiment, electromagnetic radiation interference, strong magnetic field interference, and sudden voltage and current interference in the circuit can remarkably disrupt the functioning of the experimental equipment. These interferences must be reduced or eliminated to ensure the normal operation of the equipment in an optimal environment and to obtain accurate and reliable experimental data. The following anti-interference measures were implemented.

Power supply measures: The charging and discharging system of the high-voltage pulse discharge experimental platform uses single-phase alternating current as the charging power supply. However, the charging power supply experiences pulse fluctuation interference during discharge. Both the measuring system and the notebook computer are powered by independent DC rechargeable batteries to avoid conductive coupling interference between the charging and discharging system and the measuring system via the same power supply. This setup helps eliminate crosstalk between measuring instruments and reduces interferences from pulse fluctuations.

Grounding precautions: During high-voltage pulse discharge, a pulse high voltage is generated at the grounding point of the capacitor equipment. Therefore, special attention is given to the grounding position of the test system, ensuring it is located far away from the capacitor's grounding point.

Electromagnetic shielding precautions: All measuring equipment shells are made of metal and are placed inside metal shielding boxes during measurement and data collection.

Loop inductance measurement: The loop inductance is determined by the length of the conductor. Shorter coaxial cable conductors are preferred in the experiment to reduce loop inductance.

4. Result analysis and discussion

4.1 Equivalent numerical simulation and equivalent circuit simulation of discharge breakdown

Simulation of underwater pulsed discharge breakdown can be divided into two parts: 1. Equivalent numerical simulation of breakdown; 2. Equivalent circuit simulation of breakdown. The equivalent numerical simulation focuses on the theoretical analysis of the heating effect, providing more accurate calculations for the plasma channel model (Figure 5). The equivalent circuit simulation emphasizes the variation of the equivalent resistance throughout the discharge process and its direct impact on breakdown delay. The key correlation between the two simulations lies in the equivalent heating resistance of breakdown. An accurate description of the breakdown process of underwater pulsed discharge can be achieved by combining the two parts.

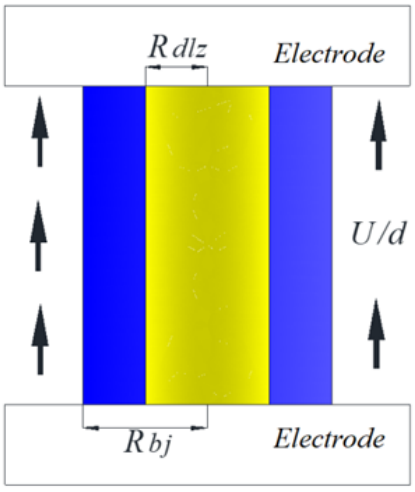

Fig. 5. plasma channel model

In Fig. 5, the yellow part represents the initial plasma channel in the gap between the two electrodes, and the blue part represents the water medium at the channel's boundary. This portion of the blue water body undergoes heating, gasification, and ionization before breakdown. *U* represents the voltage between the two electrodes, *D* represents the electrode spacing, *Rdlz* represents the initial plasma channel radius, and *Rbj* represents the distance from the channel center to the boundary of the heated water body.

4.1.1 Equivalent numerical simulation of discharge breakdown

In-depth analysis of the breakdown characteristics of underwater pulsed discharge reveals two conditions that must be met simultaneously to achieve breakdown: the water medium at the plasma boundary must be heated to approximately 500 °C [20], and the residual voltage after pre-breakdown heating must be sufficient for breakdown. Kuzhekin [21] found through experiments that the minimum field strength required for discharge breakdown is approximately 8 kV/cm, and breakdown is challenging to achieve below this value. Therefore, the threshold of the boundary water temperature for static breakdown is 773 K, and the threshold of discharge breakdown field strength is 8 kV/cm.

To analyze the behavior of the temperature T_{bj} of the boundary water medium and voltage *Ut* over time during the pre-breakdown process, we calculate their relationship curves. However, calculating the electrode gap voltage *U(t)*, which follows a similar attenuation pattern to an R-C circuit, is overly complex. Therefore, for the sake of simplification, we treat it iteratively, where $Z_{dx}(t)$ represents a constant equivalent resistance.

$$U_{n+1} = U_n\left(1-\frac{\Delta t}{CZ_{dx}}\right) \tag{1}$$

$$T_{w\_n+1} - T_{w\_0} = 23.8\int_0^t \frac{(U_{n+1})^2 G_{w\_n}}{d^2}\cdot dt + 23.8\int_0^t \left(\frac{(U_{n+1})^4}{d^4}\cdot\frac{1184.2R_{dlz}^2}{10^4\left(\frac{(U_{n+1})^2\cdot R_{dlz}}{d^2}\right)^{0.4}}\times 0.1\right)dt \tag{2}$$

where G_{w_n} represents the conductivity at different water temperatures, which can be determined using Formula (3).

The relationship between water conductivity G_w and temperature Tw is as follows [20]:

$$\begin{aligned} G_{w\_n} &= G_{w\_0} + 340\left(T_{w\_n} - 0.0283\right), T_{w\_n} \le 0.0373 \\ G_{w\_n} &= 4.26, T_{w\_n} \ge 0.0373 \end{aligned} \tag{3}$$

In Formulas (1), (2), and (3), n is an integer greater than or equal to 0. Considering the experimental conditions, we have the following values: C=60, T_{w_0}=0.0283, d=0.5, G_{w_0}≈1.2, and the charging voltage U_0=*x*, R_{dlz}=*y*, Z_{dx}=*a* (constant). The initial plasma channel radius R_{dlz} and equivalent resistance Z_{dx} are treated as an equivalent heating process, ignoring the ionization process and changes during heating. Only the heating result and residual voltage are considered to streamline the calculation process and obtain more accurate values for the "initial channel equivalent radius $R_{dlz\text{-}dx}$" and "water gap equivalent resistance Z_{dx}." This approach completely satisfies the accuracy requirements for explaining the mechanism of underwater pulsed discharge and its industrial applications (the simulation results for the initial channel equivalent radius $R_{dlz\text{-}dx}$ are graded at 0.01 m). This "equivalent approximate calculation" has a concise operational expression.

The whole iterative calculation is divided into two parts: the pre-breakdown heating part, and the non-breakdown or breakdown part. The breakdown heating part is iterated as follows, starting with Formula (1) and n=0.

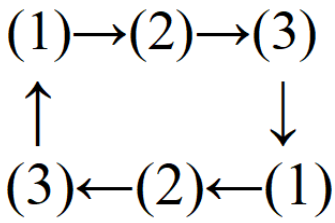

Fig. 6. Calculation process

When T_{w_n+1} obtained through iteration in Equation (2) is greater than or equal to 0.0773, the second part is executed.

Breakdown does not occur: when T_{w_n+1}≥0.0773 and U_{sy}<4 kV, the iterative calculation of Formula (1) continues, and Equations (2) and (3) are ignored until U≈0. U_{sy} refers to the calculation result of Formula (1) for U_{n+1} when T_{w_n+1}exceeds 0.0773.

When T_{w_n+1}≥0.0773 and U_{sy}> 4kV, the plasma channel forms an arc and rapidly expands after breakdown. The equivalent resistance of the water gap Z_{jc}^{dx} decreases dramatically, falling well below the characteristic impedance of the circuit. The pre-breakdown overdamped state instantly transitions to an underdamped state, and the parasitic inductance L becomes an important parameter in the whole discharge circuit. The approximate iteration formulas for an underdamped L-R-C discharge circuit are as follows:

$$I_{sy}^{n+1}=\frac{U_{sy}^{n}\Delta t-I_{sy}^{n}\left(\Delta t\right)^{2}/2C+LI_{sy}^{n}}{Z_{jc}^{dx}\Delta t+L+\left(\Delta t\right)^{2}/2C} \tag{4}$$

$$U_{sy}^{n+1}=U_{sy}^{n}-\frac{\left(I_{sy}^{n+1}+I_{sy}^{n}\right)\Delta t}{2C} \tag{5}$$

Where U_{sy}^{n} and I_{sy}^{n} represent the residual voltage and residual current after breakdown, and n is an integer greater than or equal to 0. Z_{jc}^{dx} is the equivalent resistance of the water gap after breakdown, approximately 0.1 Ω based on equivalent circuit simulations and theoretical calculations. The inductance l of the circuit is *0.000001 H (1 μH)*. Prior to the breakdown, I_{sy}^{0}=0, and U_{sy}^{0} is equal to the calculation result of Formula (1) for *Un+1* corresponding to the first portion of the simulation when Tw_n+1 exceeds 0.0773. Equations (4) and (5) are iterated until the simulation of $Usyn$≈0 is completed. The above equivalent heating analysis is programmed and calculated using Matlab software.

4.1.2 Equivalent circuit simulation of breakdown

Establishing a concise and easy-to-understand equivalent circuit structure based on experimental research and industrial applications are necessary in simulating the equivalent resistance of breakdown in underwater pulsed discharge. This allows for the analysis and interpretation of experimental results in conjunction with the equivalent numerical simulation of breakdown. After a short delay, the initial plasma channel transforms into a discharge arc channel. In terms of equivalent resistance, the channel's equivalent resistance starts off high, and then decreases sharply to a low value after a certain delay. This leads to the occurrence of a large pulse current in the arc, enabling capacitor discharge. Consequently, we simplify the complex discharge process by focusing on the analysis of equivalent resistance, which allows for a quantitative examination of discharge breakdown through simulation. Fig. 7 depicts the equivalent circuit diagram for underwater pulsed discharge.

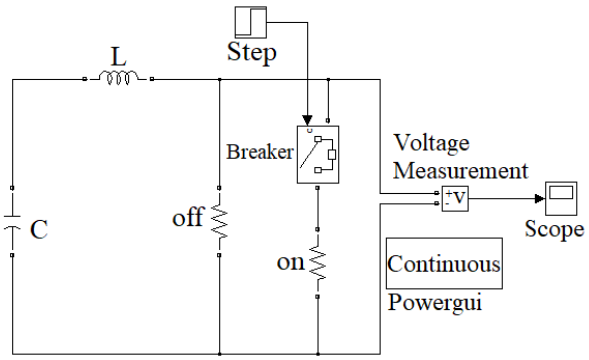

Fig. 7. Schematic of the equivalent circuit for pulsed discharge under water

In Fig. 7, "c" denotes a capacitor that is charged by an external power supply (omitted from the circuit diagram). "l" denotes the discharge circuit inductance. "off" represents the equivalent resistance of the plasma channel in the heating effect section, and "on" represents the equivalent resistance of the arc. The "Step and Breaker" component corresponds to the breakdown delay control system, and the "Voltage Measurement and Scope" component is responsible for acquiring voltage data from a the discharge water gap. The "powergui" element is used for operation debugging. The simulation programming for the equivalent circuit diagram of underwater high-voltage pulse discharge is performed using Matlab commercial computing software. The simulation is implemented using the Simulink extension of Matlab, which combines dynamic system modeling, block diagram interfaces, and interactive simulation functions. The required system model is created through module programming and module connection to facilitate simulation analysis.

4.2 Analysis of the equivalent resistance characteristics of the plasma channel

The initial plasma channel mainly exists during the stage of streamer generation, connection, and pre-breakdown, with its main purpose being to heat the boundary water medium of the initial plasma channel to a temperature of 773 K, thereby achieving breakdown. In this process, the initial channel functions similarly to a heating resistor, raising the temperature of the boundary water medium. The electric energy required to heat the initial channel's boundary water medium to a certain temperature is equivalent to the electric energy required to heat the boundary water medium directly using a resistor. Therefore, a resistor can be used as an equivalent representation of the final heating effect during breakdown, given the same heating electric energy and time (breakdown delay). This resistor is referred to as the equivalent resistance of the initial channel.

In the whole discharge circuit, the specific resistance can be analyzed through voltage measurements. Fig. 8 displays the voltage time-history curve obtained from experimental measurements.

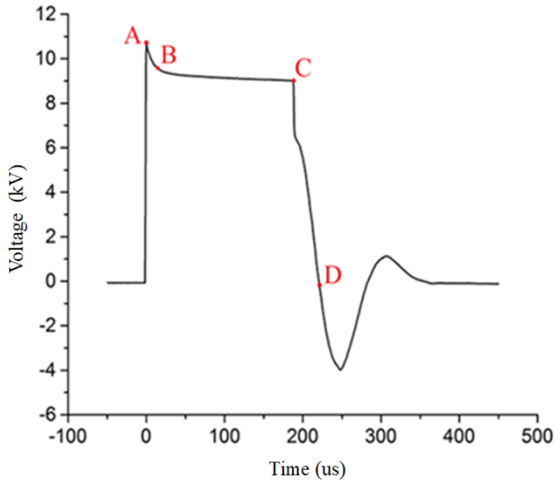

Fig. 8. Voltage time history curve

The transient voltage time-history curve shown in Fig. 8 can be divided into three sections: AB, BC, and CD, marked by points A, B, C, and D. The AB section corresponds to the streamer generation and connection stage, the BC section represents the pre-breakdown stage, and the CD section signifies the breakdown and arc detonation stage.

Sections AB and BC are the heating effect sections, where the plasma channel transforms into the initial channel. The slope of the voltage curve in the AB section provides insights into the resistance change of the initial channel. The high absolute value of the slope indicates a low equivalent resistance during this stage. The analysis of the mechanism reveals that the process of streamer generation and connection occurs rapidly (within 20 s) and is primarily driven by "gasification-ionization." Electron collision ionization is the main factor in streamer formation, resulting in high conductivity and rapid discharge of the capacitor voltage. The resistance heating effect is incidental, leading to a small equivalent resistance in this section. As the voltage decreases rapidly, the absolute value of the slope of the curve gradually decreases, indicating a gradual increase in resistance.

The absolute value of the slope in the BC section is extremely small, and it gradually stabilizes, suggesting and large and stable equivalent resistance in this stage. The mechanism behind this phenomenon is primarily the formation of the initial plasma channel after the streamer connects to the two poles. Having sufficient electrons in the channel is necessary for discharge breakdown because the particle density in the plasma is low, leveraging the weak expansion characteristics of the initial channel. Thus, the BC section mainly focuses on increasing the particle density in the channel by heating the boundary water medium of the gasification plasma channel. The heating effect on the equivalent resistance is particularly prominent during this stage.

During the heating effect period from the power supply activation at point A to the discharge breakdown at point C, the resistance of the initial channel gradually transitions from a small value to a large and stable value. Assuming a constant gasification energy is required to heat the boundary water medium of the initial channel in this process (determined by the quality and heating temperature of the water), the gradual resistance change can be simplified as a constant resistance, as long as the same gasification energy is applied to the boundary water medium at the same time. This equivalent simplification allows for raising the water temperature and maintaining the power of the heating effect section, whereas the residual voltage at the time of discharge breakdown at point C remains unaffected. This numerical simulation approach provides a reasonable simplification without sacrificing accuracy. Fig. 9 illustrates an equivalent diagram of the voltage-time curve shown in Fig. 8, assuming a constant value for the initial channel's equivalent resistance.

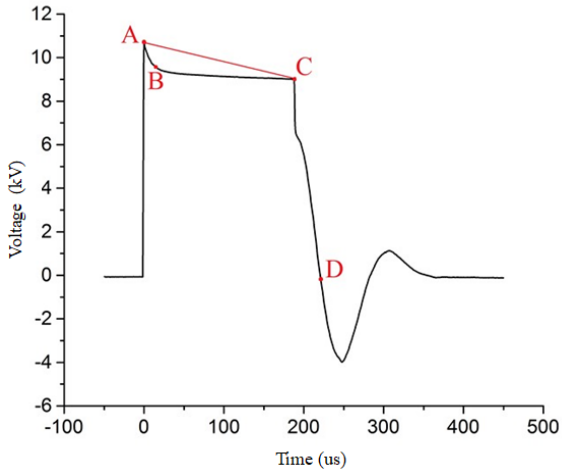

Fig. 9. Equivalent diagram of voltage time-history curve (assuming constant initial channel equivalent resistance)

In Fig. 9, the AC straight line represents the voltage change trend when the initial channel' equivalent resistance value is constant. The gradual power heating (ABC curve) corresponds to constant power heating (AC straight line) when the initial channel's equivalent resistance value is set to Z_{dx}.

In the whole discharge process, the channel resistance follows the differential equation of L-R-C loop as follows:

$$\frac{1}{C}\int idt + R(t)i + L\frac{di}{dt} = 0 \tag{6}$$

where L represents the inductance of the conductor, which is a small constant value (approximately 1 h), and C *is* the rated capacitance with a value of 60 f. $R(t)$ denotes the equivalent resistance of the water gap, and the pure resistance of the circuit is negligible. When $R(t)$ is a constant value Z_{dx}, the equivalent resistance of the initial channel is much greater than the characteristic impedance of the loop $2\sqrt{L/C}$, resulting in a non-oscillatory linear attenuation of the voltage waveform. This indicates that the circuit state is over dampened. The current expression can be derived using Equation (6).

$$i = \frac{U}{L(P_1 - P_2)}(e^{P_1 t} - e^{P_2 t}) \tag{7}$$

Where,

$P_1 = -\frac{R}{2L} + \sqrt{\frac{R^2}{4L^2} - \frac{1}{LC}}$, $P_1 = -\frac{R}{2L} - \sqrt{\frac{R^2}{4L^2} - \frac{1}{LC}}$.

At $t = \frac{\ln(P_1 / P_2)}{P_1 - P_2}$, the theoretical maximum value of current I is given by

$$I_{\max} = U \cdot \sqrt{\frac{C}{L}} \cdot e^{-\sqrt{\frac{R^2C}{R^2C-4L}} \cdot ath\left(\sqrt{\frac{R^2C-4L}{R^2C}}\right)} \approx \kappa U \cdot \sqrt{\frac{C}{L}} \tag{8}$$

where $0 \leq k \leq 1$. When the total resistance of the loop is large, the k value is approximately 0, and the current can be ignored. When the total resistance of the loop approaches 0, the k value is approximately 1, representing the under-damping situation, which will be further discussed.

In Fig. 8, the discharge breakdown occurs after time c. The arc reaches a highly ionized state and rapidly expands outward, causing the resistance of the arc channel to immediately decrease and approach zero. The arc channel resistance follows a time-varying second-order homogeneous differential equation. The equivalent resistance of the arc channel can be approximated by a fixed value denoted as Z_{jc}^{dx} due to its overall small value (less than 0.2 Ω and short arc duration).

In Equation (6), during the discharge breakdown process, the equivalent resistance $R(t) \approx Z_{jc}^{dx}$ is remarkably smaller than the characteristic impedance of the discharge circuit $2\sqrt{L/C}$, resulting in an under-damped circuit state with rapid oscillation attenuation. The current I vibration attenuation is described by Equation (9).

$$i = \frac{U}{\sqrt{\frac{L}{C} - \frac{R^2}{4}}} e^{-\alpha \cdot t} \sin \beta t = \frac{U}{L\beta} \cdot e^{-\alpha \cdot t} \cdot \sin \beta t \tag{9}$$

Where,

$$\alpha = R/2L \ , \ \beta = \sqrt{\frac{1}{LC} - \frac{R^2}{4L^2}} \ .$$

If r approaches 0, then α also approaches 0, and the theoretical maximum value of current I can be obtained using Equation (10).

$$I_{\max} = U\sqrt{\frac{C}{L}} \tag{10}$$

Calculating Equations (8) and (10) reveals that when the initial channel's equivalent resistance constant value Z_{dx} in the AC section of Figure 9 is extremely high, no current output is observed. However, the resistance of the arc channel in the CD segment and beyond is extremely low, which results in the output of a large pulse current and obvious oscillation due to the presence of loop inductance. Fig. 10 shows the time-history curve of the discharge current measured in an experiment.

The current time-history graph in Fig. 10 and the voltage time-history graph in Fig. 8 are measured in the same experiment, and the corresponding time and physical meaning of the four points A, B, C, and D in the figures are consistent. In Fig. 10, the AC section represents a heating effect section, and the corresponding current is 0, which aligns with the theoretical analysis result from the overdamped state current Equation (8). The current in the CD section suddenly rises to its peak value, which is consistent with the theoretical analysis result from the current Equation (10) in the underdamped state. The initial channel's equivalent resistance and the breakdown arc's equivalent resistance, when assumed as fixed values, closely approximate the experimental results. This indicates that the initial channel's equivalent resistance Z_{dx} and the breakdown arc's equivalent resistance Z_{jc}^{dx} can approximate the entire discharge breakdown process, providing a solid theoretical foundation for analysis and simplifying numeric calculations.

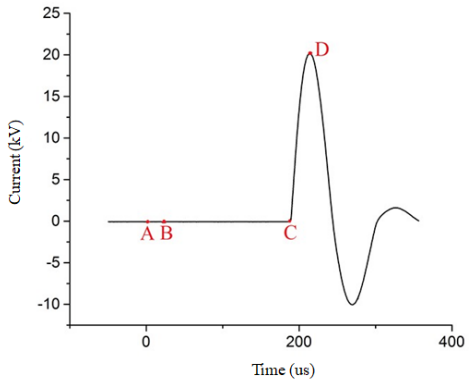

Fig.10. Time-history curve of discharge current

4.3 Theoretical analysis of the equivalent radius of the plasma channel

The streamer extending from one electrode end to the other forms the plasma channel, which is referred to as the initial plasma channel in the heating effect section but can also be referred to as the initial channel. The plasma channel is known as the arc channel after the discharge breakdown stage. The resistance characteristics of the discharge water gap have been examined, and it is established that the plasma channel can be approximated as a resistor. The factors affecting its resistance can be roughly divided into three points: 1. the resistor's material, 2. its length (which equals the electrode spacing), and 3. its cross sectional radius (which equals the plasma channel's cross sectional radius.

The equivalent resistance material is predetermined when studying different equivalent resistance values under the same discharge equipment and charging voltage (the field strength determines the degree of channel ionization, and the field strength before breakdown is relatively stable), and the electrode spacing is also stable. Therefore, the cross sectional radius of the plasma channel has the greatest influence on the resistance characteristics of the water gap.

The general change process of the cross-section radius of plasma channel is as follows: during the initial stage of the plasma channel formation, the cross section radius of the channel develops in the range of μm to 10^{-1} μm. As the electrode voltage decreases, the channel's cross section gradually shrinks and approaches a certain value, causing the equivalent resistance of water gap to increase to a certain value (the change in slope of the ABC curve in Fig. 7 illustrates the phenomenon of channel cross section shrinking). After a prolonged breakdown delay, the discharge breakdown occurs. At this time, the radius of the plasma channel instantly expands to the order of 10^2 μm and increases rapidly, but the duration is short. This process also corresponds to the under damped state mentioned above, where the equivalent resistance is extremely small, close to zero.

The plasma channel remains in a gradual state throughout the discharge process. However, accurately measuring the specific value of the plasma channel and quantifying the entire process of the change of the cross sectional radius change is challenging due to its microscopic nature (extremely short time and small channel size). Therefore, the concept of equivalent resistance can be used to quantitatively describe the cross sectional radius of a plasma channel and the channel's cross sectional radius can be divided into two parts: the heating effect section and the breakdown detonation section.

Initially, the cross section radius of the initial plasma channel in the heating effect section gradually shrinks and approaches a certain value, resulting in a stable channel radius. In conjunction with the fixed value of the initial channel equivalent resistance Z_{dx} discussed in Section 3.1, the cross section radius of the initial channel can be approximated as a fixed value, which corresponds to the equivalent resistance Z_{dx}. This fixed value represents the initial channel's equivalent radius and enables a stable heating process under this radius. In other words, it is referred to as the initial channel equivalent radius R_{dlz_dx} to describe the characteristics of the initial channel radius more intuitively and concisely. This approximation allows for streamlined numerical calculations and theoretical analysis, simplifying the overall analysis process.

In the heating effect section, the cross section of the initial channel gradually decreases because of voltage decrease at both ends of the electrode. This indicates that the initial channel's equivalent radius R_{dlz_dx} corresponds to a stable voltage value, ensuring a constant channel radius. This stable voltage represents the equivalent heating power of the AC straight line in Fig. 9 (using the equivalent resistance Z_{dx}). Therefore, R_{dlz_dx} is marked at the midpoint of the AC straight line, where the corresponding voltage value is located. In the actual process, the BC segment represents the primary stage of plasma channel existence, and the AB segment within the AC segment involves a specific process of initial channel conduction formation. As stated previously, a constant channel section radius R_{dlz_BC} is assumed in the BC section, which represents the heating effect of the BC section. The specific voltage corresponding to this constant value R_{dlz_BC} is marked at the midpoint of the BC straight line. Fig. 11 illustrates the labeling diagram of the initial channel equivalent radius R_{dlz_dx} and the BC channel equivalent radius R_{dlz_BC}.

In Fig. 11, R_{dlz_dx} and R_{dlz_BC} are marked. Point B represents the moment when the streamer passes through the two poles, forming an initial plasma channel. At this time, the initial section radius of the initial channel is R_{dlz_B}. Point C represents the end time of the initial channel, which occurs when the channel boundary temperature reaches the breakdown condition. The corresponding channel cross section radius is R_{dlz_C}. R_{dlz_B} and R_{dlz_C} are transient values, whereas R_{dlz_dx} and R_{dlz_BC} are fixed values. However, the slope of their curves can be used to determine the relationship between the channel cross sectional radii, from which $R_{dlz\_B} > R_{dlz\_dx} > R_{dlz\_BC} > R_{dlz\_C}$ can be derived. In the analysis of the entire equivalent heating process (AC section), the initial channel equivalent radius R_{dlz_dx} fully characterizes the heating effect section, leading to more concise and efficient numerical simulations and theoretical analysis. This represents the primary research objective of static breakdown equivalent heating. When considering only a single physical problem (BC pre-breakdown stage) after the formation of the initial channel, without involving the conduction and connection problems of the AB-section column, the equivalent radius of the BC-section channel R_{dlz_BC} exhibits good mean value characteristics. It is an essential parameter for the simple study of BC-section pre-breakdown and will be studied separately in future research.

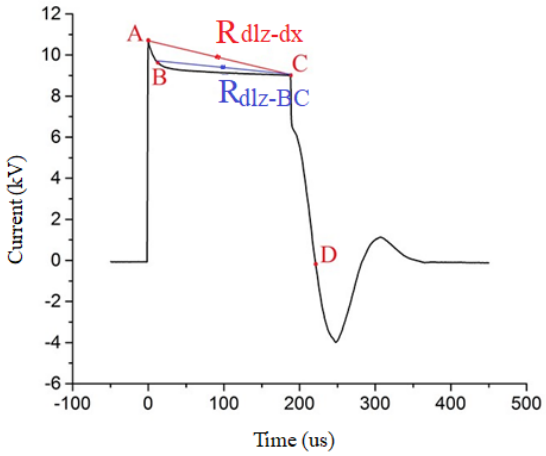

Fig. 11. R_{dlz_dx} and R_{dlz_BC} labeling diagram

The initial channel equivalent radius R_{dlz_dx} plays an important role in the heating effect section because it remarkably affects the heating efficiency of the equivalent process. However, in the breakdown and detonation section, the research on the cross section size of the plasma channel holds minimal importance. This is because the equivalent resistance of the water gap in this section is close to zero, and the process duration is extremely short. At the moment of breakdown, the arc cross section radius increases several times and continues to expand rapidly. In this process, the focus of research shifts to the transformation analysis of electric energy and mechanical energy injected into the arc channel rather than the arc cross section radius. Therefore, studying the equivalent radius of the initial channel in the heating effect section is crucial for solving field engineering discharge monitoring.

4.4 Numerical simulation and simulation analysis of discharge breakdown

The above theoretical analysis reveals that the realization of breakdown requires a heating effect. Initially, the boundary water medium of the plasma channel undergoes heating and gasification to reach a certain temperature. Simultaneously, maintaining the average electric field intensity in the electrode gap is crucial in sustaining the gasification-ionization cycle within the channel. The minimum field strength required for discharge breakdown is approximately 8 kV/cm, and achieving breakdown below this threshold becomes challenging. These factors are indispensable for the breakdown detonation process, which distinguishes it from other forms of discharge. Therefore, the breakdown process of discharge is analyzed through numerical simulation and circuit simulation.

The numerical simulation of static breakdown is discussed. The equivalent circuit simulation of static breakdown allows for an accurate calculation of the initial channel's equivalent resistance setting Zdx and the breakdown arc's resistance setting $Zjcdx$. Fig. 11 illustrates an example of the simulation based on the equivalent Fig. 8. When the charging voltage Um, the residual voltage Ub at breakdown time, and the breakdown delay tb (following the expression of Touya [22]) are consistent, the simulation results are shown in Figure 12.

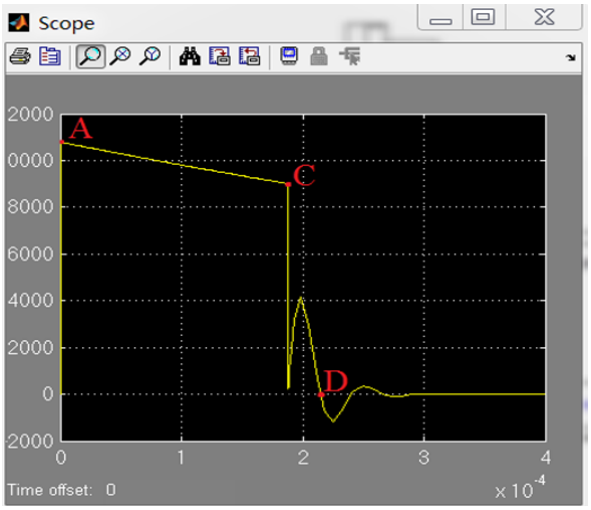

Fig. 12. Equivalent circuit simulation diagram

The equivalent circuit simulation diagram closely resembles the experimental voltage time-history curve in Fig. 9. The linear slope of the AC section, the duration of the CD section, and the curve fluctuations after time d are highly consistent. The discharge power of the AC and CD sections aligns with the experimental conditions, and the circuit simulation accurately reflects the heating effect section, the breakdown and detonation section, and the circuit under-damping fluctuation after discharge. This demonstrates that the equivalent circuit simulation can effectively capture the electrical characteristics of underwater pulsed discharge. The simulation yields the initial channel's equivalent resistance as Z_{dx}=17.35 Ω and the breakdown arc resistance as Z_{jc}^{dx} =0.096Ω. These equivalent values accurately and quantitatively reflect the discharge characteristics, providing a solid foundation for analyzing the mechanism of the pulse discharge process under hydrostatic pressure compared with the rough range of the water gap resistance provided by previous studies. During the 9–15 kV discharge breakdown process, the fixed value of breakdown arc resistance Z_{jc}^{dx} is extremely small and consistent. In circuit simulation, setting it to a fixed value of 0.1 Ω has minimal effect on the overall simulation process and can be ignored.

In conjunction with the simulation results obtained from the equivalent circuit and the theoretical analysis of the initial channel's equivalent radius, microscopic simulation of underground water pulsed discharge can be conducted through numerical simulation of static breakdown. This enables the determination of the equivalent radius of the initial channel under various discharge conditions, providing a solid foundation for analyzing the theoretical and experimental results of underground water pulsed discharge. Fig.13 serves as a legend for the numerical simulation of static breakdown corresponding to Fig. 9.

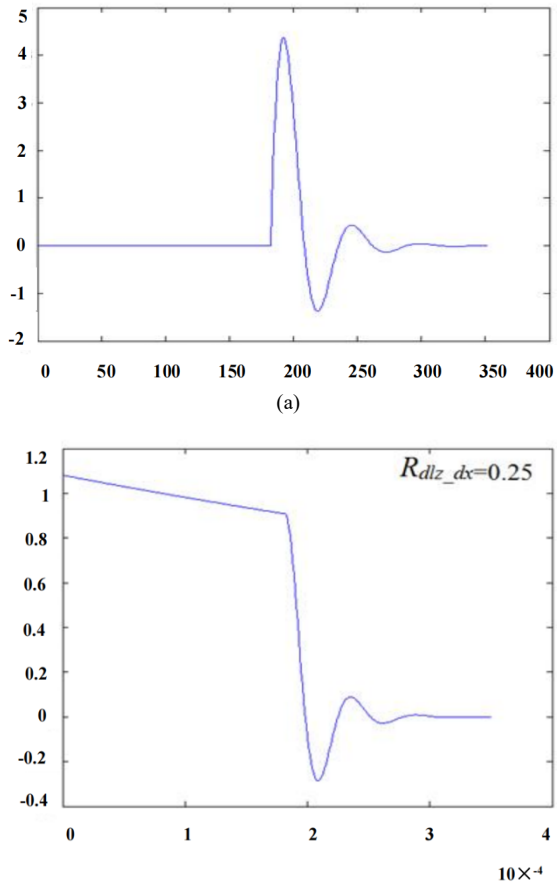

Fig. 13. Numerical simulation of breakdown theory

In Figure 13, (a) represents the simulated voltage (U)-time (t) curve, with time (t) in seconds and voltage U in units of 10^4 V. (b) represents the simulated current (I) versus (t) curve, with the horizontal axis representing time t in s and the vertical axis representing current I in 10^4 A. The numerical simulation results in Fig. 13 closely match the experimental results in Figs. 8 and 9, and the equivalent circuit simulation diagram (Fig. 12). This indicates a high degree of consistency in terms of charging voltage U_m, remaining voltage U_b at breakdown, breakdown delay t_b, and waveform fluctuation characteristics. On the basis of the results of the equivalent circuit simulation and static breakdown equivalent numerical simulation, this equivalent heating model demonstrates good accuracy in simulating the electrical characteristics of underwater pulsed discharge. Additionally, it verifies the "gasification-ionization" theory by revealing a substantial water heating process during the pre-breakdown stage. In the simulation results shown in Fig. 12, the corresponding initial channel's equivalent radius R_{dlz_dx} is 0.25 μm.

We can effectively quantify the description of the electrical characteristics of underwater pulsed discharge by introducing the theory of initial channel equivalent resistance Z_{dx} and initial channel equivalent radius R_{dlz_dx}. This allows for a more intuitive analysis of external factors influencing high-voltage pulse discharge and a more comprehensive explanation of the underlying mechanism causing these external factors.

The phenomenon of static breakdown not being achieved by over-pulse discharge, known as corona discharge, is discussed in the previous theoretical analysis and practical

experiments. Corona discharge is characterized by considerable ultraviolet radiation and finds applications in industries, such as sewage treatment, but it is not the primary focus of static breakdown research. When the average electric field intensity in the water gap falls below 8 kV/cm, sustaining avalanche ionization in the plasma channel and achieving breakdown becomes difficult [21]. Achieving breakdown becomes difficult when the theoretical breakdown residual voltage U_b is less than 4 kV because the electrode spacing in the experiment is 0.5 cm. Through this experiment, achieving breakdown is challenging when the charging voltage U_m is lower than 5.5 kV. Therefore, the characteristics of pulse discharge without static breakdown are briefly discussed through experimental figures and simulations.

A voltage experiment legend without static breakdown is shown in Fig. 14. The voltage equivalent numerical simulation results without static breakdown are shown in Figure 15. The simulation results of an equivalent circuit without static breakdown are shown in Fig. 16.

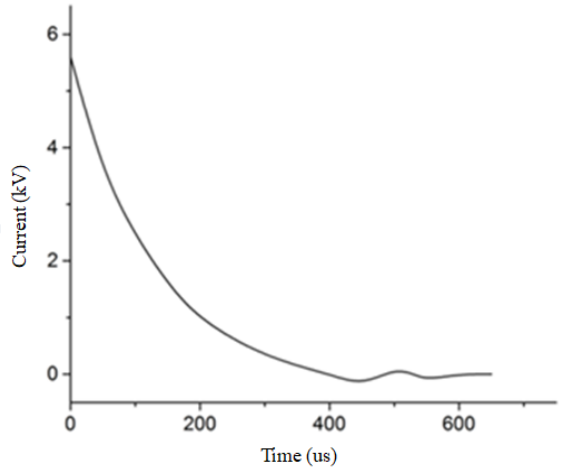

Fig.14. Voltage experimental graph depicting unrealized static breakdown

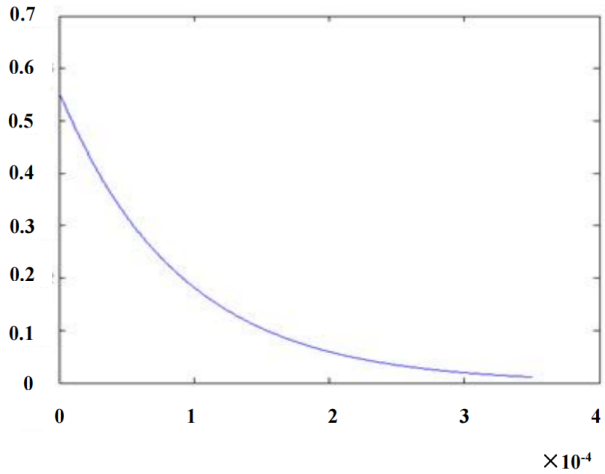

Fig.15. Equivalent numerical simulation diagram illustrating unrealized static breakdown

The experimental results show that the voltage gradually decreases to zero throughout the whole discharge process without static breakdown. The equivalent numerical simulation and simulation results closely resemble the actual experimental situation. In the case of discharge simulation without static breakdown, the whole process is equivalent to continuous radiation heating. Once the temperature of the water at the plasma boundary reaches the breakdown condition, the electric field strength in the water gap is insufficient to support the breakdown process. Thus, the breakdown cannot be achieved, and the radiation heating continues until the end of discharge, with minimal breakdown current. The main reason for the failure of breakdown is the insufficient breakdown field strength, which is attributed to a low charging voltage, similar to the findings in Yang's experimental results [23]. Therefore, in experiments studying the static breakdown of underwater pulsed discharge, the charging voltage should be higher than the threshold of 5.5 kV. The research group found that the static breakdown phenomenon can be essentially achieved when the charging voltage exceeds 6 kV.

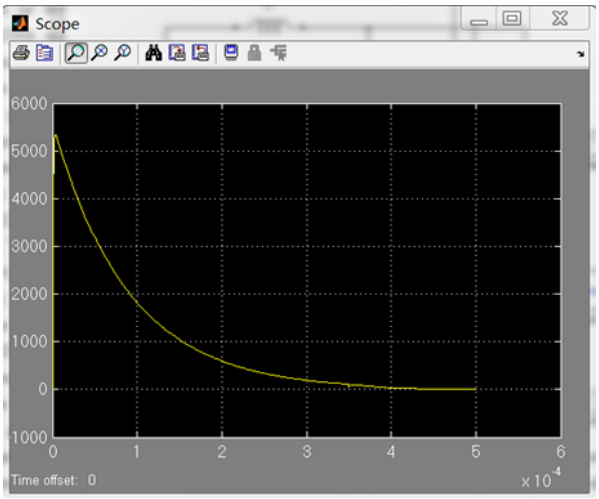

Fig.16. Equivalent circuit simulation diagram demonstrating unrealized static breakdown

5. Conclusion

This study explored the electrical energy conversion characteristics of underwater high-voltage pulsed discharge by analyzing the thermal effects, breakdown detonation characteristics, and mechanical energy conversion in the process of underwater high-voltage pulsed discharge. It revealed the entire breakdown process and the effect of the plasma channel utilizing a physical model of high-voltage pulse discharge breakdown in water, this study conducted experimental research combined with theoretical analysis. The conclusions can be summarized as follows:

(1) The breakdown channel first undergoes through the stage of an initial plasma channel, where heating effects occur. Once the heating effects are completed, the initial plasma channel transitions into an arc channel, where breakdown and detonation phenomena occur.

(2) The equivalent resistance of the plasma channel is approximately 10 Ω, and the initial channel's equivalent radius is around 0.1 μm. Experimental observations and theoretical simulations have shown that achieving breakdown with an electrode gap of 0.5 cm and a charging voltage Um below 5.5 kV is challenging. A minimum charging voltage of approximately 6 kV is required to achieve breakdown.

(3) On the basis of equivalence theory, quantifying the equivalent radius and equivalent resistance during the breakdown process provides a representative method for describing the stability of the breakdown process. This approach proves effective in monitoring the operation of discharge equipment in practical engineering applications.

This study combines indoor experiments with theoretical research and proposes an equivalent theoretical and numerical simulation model for breakdown in underwater high-voltage pulsed discharge. The constructed plasma model is simpler and more realistic, providing a reliable reference for the future development of underground water high-voltage pulsed discharge technology and performance monitoring evaluations. However, the study is limited because of the lack of plasma monitoring methods and insufficient data on high-temperature and high-pressure plasma. Future work will require advanced experimental equipment and methods to investigate the thermal effects and laws of mechanical energy conversion during the breakdown process.

Acknowledgements

This work was sponsored by the National Natural Science Foundation of China (Grant No.52279134)；Sponsored by Natural Science Foundation of Henan (Grant No. 232300420323); Sponsored by Nanhu Scholars Program for Young Scholars of Xinyang Normal University.

This is an Open Access article distributed under the terms of the Creative Commons Attribution License.

References

[1] T. Zhu, L. Yang, Z. Jia, and Q. Zhang, "Characteristics of streamer discharge development between the dielectric-coated sphere-plane electrodes in water," *J. Appl. Phys.*, vol. 104, no. 11, Dec. 2008, Art. no.113302.

[2] J. F. Kolb, R. P. Joshi, S. Xiao, and K. H. Schoenbach, "Streamer in water and other dielectric liquids," *J. Phys. D: Appl. Phys.*, vol. 41, no. 23, Sep. 2008, Art. no.234007.

[3] G. Touya, T. Reess, L. Pecastaing, A. Gibert, and P. Domens, "Development of subsonic electrical discharges in water and measurements of the associated pressure waves," *J. Phys. D: Appl. Phys.*, vol. 39, no. 24, pp. 5236–5244. Oct. 2006.

[4] W. Chen, O. Maurel, T. Reess, A. S. De Ferron, and C. La Borderie, "Experimental study on an alternative oil stimulation technique for tight gas reservoirs based on dynamic shock waves generated by Pulsed Arc Electrohydraulic Discharges," *J. Petrol. Sci. Eng.*, vol. 88, no. 89, pp. 67-74. Jun. 2012.

[5] P. Bruggeman and C. Leys, "Non-thermal plasmas in and in contact with liquids," *J. Phys. D: Appl. Phys.*, vol. 42, no. 5, Jan. 2009, Art. no. 053001.

[6] A. Hamdan, J. Diamond, and A. Herrmann, "Dynamics of a pulsed negative nanosecond discharge on water surface and comparison with the positive discharge," *J. Phys. Commun.*, vol. 5, no. 3, Mar. 2021, Art. no. 035005.

[7] A. Hamdan, D. A. Ridani, J. Diamond, and R. Daghrir, "Pulsed nanosecond air discharge in contact with water: influence of voltage polarity, amplitude, pulse width, and gap distance," *J. Phys. D: Appl. Phys.*, vol. 53, no. 35, Jun. 2020, Art. no. 355202.

[8] C. Rond, J. M. Desse, N. Fagnon, X. Aubert, and M. Er, "Time-resolved diagnostics of a pin-to-pin pulsed discharge in water: pre-breakdown and breakdown analysis," *J. Phys. D: Appl. Phys.*, vol. 51, no. 31, Jul. 2018, Art. no. 335201.

[9] T. Merciris, F. Valensi, and A. Hamdan, "Determination of the Electrical Circuit Equivalent to a Pulsed Discharge in Water: Assessment of the Temporal Evolution of Electron Density and Temperature," *IEEE T Plasma Sci.*, vol. 48, no. 9, pp. 3193 - 3202. Aug. 2020.

[10] R. J. Wandell, H. Wang, K. Tachibana, B. Makled, and B. R. Locke, "Nanosecond pulsed plasma discharge over a flowing water film: Characterization of hydrodynamics, electrical, and plasma properties and their effect on hydrogen peroxide generation," Plasma Process Polym., vol. 15, no. 6, Feb. 2018, Art. no. 1800008.

[11] X. Lu, Y. Pan, K. Liu, M. Liu, and H. Zhang, "Spark model of Pulsed discharge in water," J. Appl. Phys., vol. 90, no. 1, pp. 24-31. Jan. 2002.

[12] X.P. Lu *et al.*, "A cold plasma cross made of three bullet-like plasma plumes," *Thin Solid Films.*, vol. 518, no. 3, pp. 967-970. Jul. 2009.

[13] D. Ye, Y. Yu, L. Liu, X. Lu, and Y. Wu, "Cold plasma welding of polyaniline nanofibers with enhanced electrical and mechanical properties," *Nanotechnol.*, vol. 26, no. 49, Nov. 2005, Art. no. 495302.

[14] Y. Li, Y. Sun, Y. Liu, L. Zhang, and J. Zheng, "Electrohydraulic effect and sparker source: current situation and prospects," *High Volt.*, vol. 47, no. 3, pp. 753–755. Oct. 2021.

[15] A. Fan, Y. Sun, and X. Xu, "High-voltage pulse discharge seismic source and Its characteristics," *High Volt.*, vol. 44, no. 3, pp. 890-895. 2018.

[16] R. Fu, Y. Sun, X. Xu, and P. Yan, "Effect of hydrostatic pressure on fracture of rock subjected to plasma impact," *Combust. Explo. Shock Waves,* vol. 38, no. 5, pp. 1051–1056. Sep. 2018.

[17] H. Zhou, Y. Zhang, H. Li, R. Han, and Y. Jing, "Generation of electrohydraulic shock waves by plasma-ignited energetic materials: III. Shock wave characteristics with three discharge loads," *IEEE T. Plasma Sci.*, vol. 42, no. 12, pp. 4017-4023. Sep. 2015.

[18] L. Duan, S. Rao, D. Wang, K. Zhang, and H. Cao, "Understanding of TiO2 catalysis mechanism in underwater pulsed discharge system: Charge carrier generation and interfacial charge-transfer processes," *Chemosphere.*, vol. 267, Dec. 2021, Art. no. 129249.

[19] D. Yan, D. Bian, J. Zhao, and S. Niu, "Study of the electrical characteristics, shock-wave pressure characteristics and attenuation law based on pulse discharge in water," *Shock Vib.*, Mar. 2016, Art. no. 6412309.

[20] Y. Wang, "Theoretical and experimental study of plasma sound sources in water," Ph.D. dissertation, Dept. EISAT., Natl. Univ. Def. Tech., Changsha, China, 2012.

[21] I. P. Kuzhekin, "A study of breakdown of a liquid in a non-uniform field under rectangular voltage waves," *J. Tech. Phys.*, vol. 36, no. 12, pp. 2125-2130. Dec. 1966.

[22] G. Touya, T. Reess, L. Pecastaing, A. Gibert, and P. Domens, "Development of subsonic electrical discharges in water and measurements of the associated pressure waves," *J. Phys. D: Appl. Phys.*, vol. 39, no. 24, pp. 5236-5244. Oct. 2006.

[23] B. Yang, M. Zhou, and L. Lei, "Synergistic effects of liquid and gas phase discharges using pulsed high voltage for dyes degradation in the presence of oxygen," *Chemosphere.*, vol. 60, no. 3, pp. 405-411. Feb. 2005.